

## Multiple testing strategy for the detection of temporal irreversibility in stationary time series

Karina R. Casali,<sup>1,2,\*</sup> Adenauer G. Casali,<sup>2</sup> Nicola Montano,<sup>2</sup> Maria Claudia Irigoyen,<sup>1</sup> Fabricio Macagnan,<sup>3</sup> Stefano Guzzetti,<sup>4</sup> and Alberto Porta<sup>5,†</sup>

<sup>1</sup>Physiology Department, Federal University of Rio Grande do Sul, Porto Alegre, Brazil

<sup>2</sup>Department of Clinical Sciences "L. Sacco," University of Milan, Milan, Italy

<sup>3</sup>Pontifical Catholic University of Rio Grande do Sul, Porto Alegre, Brazil

<sup>4</sup>Internal Medicine II, L. Sacco Hospital, Milan, Italy

<sup>5</sup>Department of Technologies for Health, Galeazzi Orthopaedic Institute, University of Milan, Milan, Italy

(Received 21 March 2007; revised manuscript received 20 November 2007; published 6 June 2008)

We propose a strategy for the detection of temporal irreversibility in stationary time series based on multiple bidimensional tests. The test is helpful to evaluate the displacement of irreversibility toward high dimensions. The test can be used independently of the theoretical functionals actually utilized to check irreversibility. The method was applied to simulated nonlinear signals generated by the delayed Henon map and a two-loop negative feedback model to show how the presence of a delay could produce the displacement of irreversibility toward higher dimensions. The method was applied also to series of a biological variable (i.e., heart period) that is known to be regulated by multiple feedback loops. Simulations and real data support the need of exploring progressively increasing embedding dimensions when assessing temporal irreversibility.

DOI: [10.1103/PhysRevE.77.066204](https://doi.org/10.1103/PhysRevE.77.066204)

PACS number(s): 05.45.Tp, 05.70.Ln, 87.19.Hh

Among several aspects of a time series that can be quantified, time irreversibility has recently gained attention in biology and medicine [1,2]. This attention is simply the result of the ability of time irreversibility analysis to detect nonlinear dynamics [3,4], and indicates the existence of disequilibrium states [5], i.e., two fundamental properties of living dynamical systems.

In time series analysis, a signal is said to be reversible if its statistical properties are invariant with respect to time reversal, otherwise it is said to be irreversible. From this definition, reversible time series have the joint probability of  $(x(i), x(i+1), \dots, x(i+L-1))$  indistinguishable from that of  $(x(i+L-1), x(i+L-2), \dots, x(i))$ , where  $L$  is the embedding dimension.

Usually time irreversibility tests have been devised in low-dimensional phase spaces, basically by comparing the distribution of points in the plane  $(x(i), x(i+1))$  to that in the plane  $(x(i+1), x(i))$  [6–10]. However, dynamics might be roughly reconstructed in a low-dimensional phase space because complex patterns cannot be completely unfolded, and, accordingly, low-dimensional irreversibility tests may lead to unreliable results especially when dealing with high-dimensional systems such as those including delays [11].

Few times irreversibility analysis has been carried out in a dimensional phase space  $(x(i), x(i+1), \dots, x(i+L-1))$  with  $L > 2$  and in these applications  $L$  has been fixed to arbitrary values (i.e.,  $L=4$  or  $5$ ) [2,4], thus preventing one from understanding the information that can be derived when  $L$  is progressively increased.

In the cardiovascular system, regulations are usually performed via multiple feedback loops incorporating different delays [12,13], thus leading to systems that can be high dimensional and might show time scales characterized by dif-

ferent dynamical properties including a different degree of time irreversibility. In this study we propose a multiple testing strategy for the detection of temporal irreversibility in time series. The test is helpful to evaluate the displacement of irreversibility toward high dimensions. The test can be used independently of the theoretical functional actually utilized to check irreversibility (among all present in literature [6–9], here we utilized the one proposed in [9]). The method was applied to simulated nonlinear signals generated by the delayed Henon map and a two-loop negative feedback model [14] to show how the presence of a delay could produce the displacement of irreversibility toward higher dimensions and to highlight the possibility of the coexistence of time scales with different degrees of irreversibility.

In terms of real data, we tested high-dimensional irreversibility in heart period ( $T$ ) beat-to-beat series known to be regulated by nonlinear multiple delayed feedback loops (the most relevant over short time scales is baroreflex) [12,15,16] under experimental conditions altering the baroreflex delay [17,18] in the beat-to-beat domain.

### I. IRREVERSIBILITY TEST

Given a stationary time series  $x = \{x(i), i=1, \dots, N\}$  and the series of vectors  $x_L = \{(x(i), x(i+\tau), \dots, x(i+(L-1)\tau)), i=1, \dots, N-(L-1)\tau\}$ , constructed using the technique of the delayed coordinates [19],  $x$  is said to be reversible if the probability distribution of  $x_L$  is not significantly different from that of  $x'_L = \{(x(i+(L-1)\tau), \dots, x(i+\tau), x(i)), i=1, \dots, N-(L-1)\tau\}$ , obtained after reversing time's arrow in each vector  $x_L(i)$ . This should hold for any  $L$  and any  $\tau$ . In this work we used  $\tau=1$  without any *a priori* assumption regarding the dimension  $L$ .

Most of the irreversibility tests [6–9] are devised for  $L=2$  [i.e., they consider points in the plane  $(x(i), x(i+1))$ ]. The common feature of all tests is that the detection of irreversibility is based on the evaluation of asymmetry of the data

\*rabellocasali@gmail.com

†alberto.porta@unimi.it

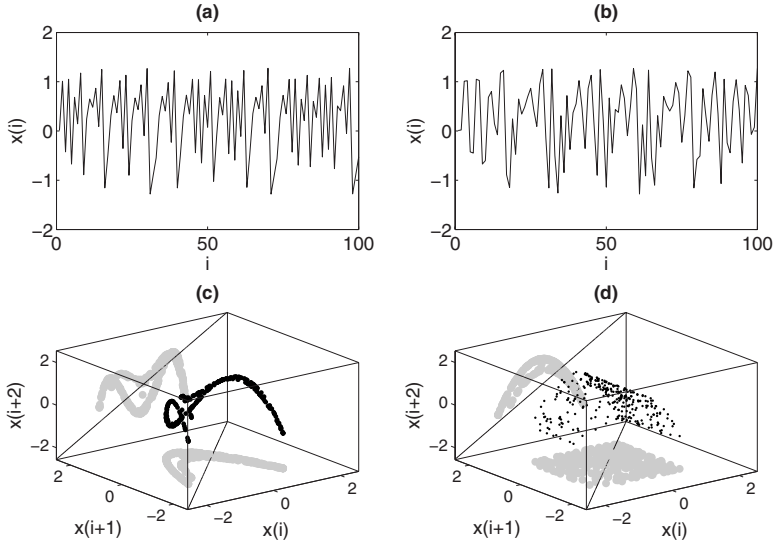


FIG. 1. Realizations of 100 samples of  $x$  computed from zeroth-order (a) and first-order (b) DHMs. Reconstruction of the dynamics of  $x$  derived from zeroth-order (c) and first-order DHMs (d) in the phase space  $(x(i), x(i+1), x(i+2))$  (black circles). The projections of the dynamics onto the planes  $(x(i), x(i+1))$  and  $(x(i), x(i+2))$  are marked with gray circles. In the case of zeroth-order DHM projections onto the planes  $(x(i), x(i+1))$  and  $(x(i), x(i+2))$  are both asymmetric with respect to the main diagonal of the plane, while in the case of first-order DHM only the projection onto  $(x(i), x(i+2))$  can reveal the asymmetry.

distribution in the plane  $(x(i), x(i+1))$  with respect to the main diagonal line  $x(i)=x(i+1)$  [7]. Indeed, by definition, this asymmetry is incompatible with time reversibility. Our study uses the correspondence between time irreversibility and asymmetry of the distribution to introduce a test of time irreversibility in stationary high-dimensional series.

Let us consider the plane  $(x(i+m), x(i+n))$  with  $m, n = 0, \dots, L-1$  and  $m \neq n$  and denote with  $d_{m,n}(i)$  the distance between the point  $(x(i+m), x(i+n))$  and the main diagonal  $x(i+m)=x(i+n)$  [i.e.,  $d_{m,n}(i)=k(x(i+n)-x(i+m))$ , with  $k=2^{(-1/2)}$ ]. Our test evaluates  $L$ -dimensional irreversibility by checking the asymmetry of the distribution of points obtained by projecting the  $L$ -dimensional reconstructed dynamics onto any orthogonal reference plane  $(x(i+m), x(i+n))$ , with  $m, n = 0, \dots, L-1$ . This can be done by testing the asymmetry of the distribution of  $d_{m,n}$  for any  $n, m = 0, \dots, L-1$  and  $m \neq n$  with respect to 0. The obvious relationships  $d_{m,n}(i) = -d_{n,m}(i)$  and  $d_{m,n}(i) = d_{0,(n-m)}(i+m)$  for  $n > m$  limit the number of tests to be performed in a stationary time series to  $L-1$  (i.e., we need to test the asymmetry of the distribution of  $d_{0,m}$  with  $m = 1, \dots, L-1$ ).

Any asymmetry measure can be applied to the  $d_{0,m}$  distribution. In this study we used the skewness of  $d_{0,m}$ ,

$$S_m = \frac{\sum_{i=1}^{N-m} d_{0,m}(i)^3}{\left(\sum_{i=1}^{N-m} d_{0,m}(i)^2\right)^{3/2}}, \quad (1)$$

with  $m = 1, \dots, L-1$  [9]. When  $S_m$  is significantly different from 0 for a specific  $m$  with  $m \leq L-1$ , the series is labeled as irreversible in the  $(m+1)$ -dimensional phase space. If  $x$  is irreversible in the  $(m+1)$ -dimensional phase space, it is said to be  $L$  irreversible for any  $L > m$ .

To check if  $S_m$  is significantly different from 0 we utilized a surrogate data approach [20]. The null hypothesis is that  $x$  is generated by a linear process being reversible at least up to the dimension  $L$  eventually distorted by a static nonlinear transformation that does not alter reversibility of  $x$ . Accord-

ingly, we generated a set of 500 amplitude-adjusted Fourier transform (AAFT) surrogates [20].  $S_m$  was calculated over the surrogate data ( $S_m^s$ 's) and over the original series ( $S_m^o$ ). If  $S_m^o$  was smaller than the critical value defining the most extreme 2.5% of  $S_m^s$ 's or larger than the critical value defining the most extreme 97.5% of  $S_m^s$ 's, the null hypothesis was rejected and the series was said to be  $(m+1)$  irreversible and generally  $L$  irreversible for any  $L > m$ .

## II. SIMULATED DATA: DELAYED HENON MAP

The first type of simulation is devoted to emphasizing the need for irreversibility testing for high-dimensional dynamics generated by models including delays. We used the delayed Henon map (DHM) to generate a set of time series. The  $\sigma$ -order DHM can be written as

$$x(i+1) = 1 - ax^2(i-\sigma) + y(i-\sigma), \quad (2)$$

$$y(i+1) = bx(i-\sigma), \quad (3)$$

with  $a=1.4$ ,  $b=0.3$ , and  $i=\sigma+1, \dots, N-1$ . A nondelayed Henon map has  $\sigma=0$  and produces  $x$  that is found to be two irreversible. When the data is generated from higher-order DHM, the bidimensional irreversibility test fails to detect irreversibility. Indeed, the effect of a delay in the DHM is to displace irreversibility to higher dimensions. In Fig. 1, we plot the reconstruction of the dynamics of  $x$  in the phase space  $(x(i), x(i+1), x(i+2))$  for a zeroth-order and first-order DHM. In the case of the zeroth-order DHM, when the dynamics is projected onto the plane  $(x(i), x(i+1))$ , the points are asymmetric with respect to the main diagonal  $x(i)=x(i+1)$  [Fig. 1(c)], thus indicating that  $x$  is two-irreversible. In the case of the first-order DHM, when the dynamics is projected onto the plane  $(x(i), x(i+1))$ , the points are symmetric with respect to  $x(i)=x(i+1)$  [Fig. 1(d)], thus failing to detect irreversibility. Irreversibility can be detected only when evaluating the asymmetry of the projection of the dynamics onto the plane  $(x(i), x(i+2))$  with respect to  $x(i)=x(i+2)$ .

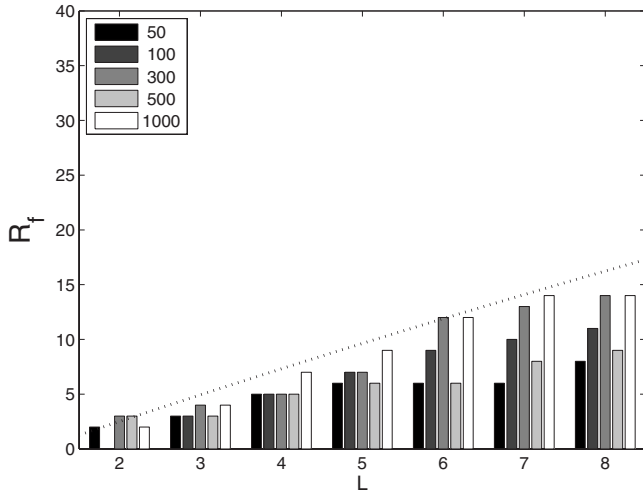


FIG. 2. Percentage of  $L$ -irreversible dynamics of the multidimensional irreversibility test relevant to 50, 100, 300, 500, and 1000 samples of WGN. Since WGN is reversible, the percentage of  $L$ -irreversible dynamics corresponds to the percentage of false rejections ( $R_f$ ). The relationship  $100 \times (1 - (1 - q_2)^{L-1})$ , where  $q_2$  is the probability of detecting two-irreversible dynamics is plotted as a dotted line.

III. SIMULATED DATA: WHITE GAUSSIAN AND COLORED NOISES

The second type of simulations was aimed at evaluating the percentage of false rejections ( $R_f$ ) of the proposed irreversibility test. We generated 500 realizations of white Gaussian noise (WGN) of various lengths. WGN is known to be reversible [21], thus we should find  $R_f=0$ . In Fig. 2 we plot  $R_f$  in the case of WGN realizations with  $N=50, 100, 300, 500,$  and  $1000$  as a function of  $L$ . It is worth noting that  $R_f$  is rather independent on  $N$ .

If  $q_{m+1}$  is the probability for a reversible signal to be detected as irreversible in the  $(x(i), x(i+m))$  projection of the dynamics, the probability of a reversible signal to be found  $(m+1)$  irreversible without rejecting the null hypothesis for lower dimensions is  $q_{m+1} \prod_{k=2}^m (1 - q_k)$ . Under the approximation that  $q_k$  is independent of the index  $k$ , i.e.,  $q_k = q_2 \forall k \in \{2, \dots, L\}$ , we can estimate the  $R_f$  for an  $L$ -dimensional test as  $1 - (1 - q_2)^{L-1}$ . This relationship (multiplied by 100) is plotted in Fig. 2 (dotted line), showing that the estimated expression acts, indeed, as an upper bound to our data. Clearly,  $R_f$  increases as a function of  $L$  (i.e., it is more likely to have erroneous detection of  $L$ -irreversible dynamics when  $L$  is large). Hence, it is important to select a theoretical functional (here S) and/or to increase the level of confidence of the surrogate data test in order to have a small  $q_2$ . In this study, with a confidence level of 95%,  $q_2$  was about 2.5%. Therefore, in order to have  $R_f \leq 10\%$ , we limited  $L$  to 5, which is believed to be high for short heart rate variability data [22]. In general, the largest  $L$  that can be reliably explored can be derived by solving the equation  $1 - (1 - q_2)^{L-1} = p$  after evaluating  $q_2$ , where  $p$  is the probability of having a type I error in a multiple testing strategy. Usually  $p$  is set to 0.05.

We tested  $R_f$  over colored processes obtained by filtering WGN realizations with a transfer function with two complex

TABLE I. Percentage of true rejections of the multidimensional irreversibility test applied to first-order DHM (300 samples) corrupted with WGN of different standard deviations (i.e., 0%, 50%, 100%, and 150% of the standard deviation of the uncorrupted first-order DHM realization).

	$L=3$	$L=4$	$L=5$	$L=6$	$L=7$
0	100	100	100	100	100
50	100	100	100	100	100
100	86	87	87	89	90
150	58	61	62	63	65

and conjugated poles with modulus equal to 0.9 and phases equal to  $\pm \pi/5$  or phases equal to  $\pm 3\pi/5$ , thus generating autoregressive processes. In the former case we simulated a process with a dominant slow oscillation, whereas in the latter case we simulated a process with a dominant fast oscillation (with a sampling frequency of 1 Hz, the pole frequency is 0.1 Hz or 0.3 Hz, i.e., the frequencies of the usual dominant oscillations present in heart rate variability). The course of  $R_f$  relevant to autoregressive process with slow dynamics was not significantly different from that derived from WGN (Fig. 2), while that relevant to the faster autoregressive dynamics had the same rate of increase as WGN but  $q_2$  was 30% higher.

IV. SIMULATED DATA: DELAYED HENON MAP CORRUPTED BY NOISE

The third type of simulations aimed at evaluating the percentage of true rejections ( $R_t$ ) of the proposed irreversibility test. We added WGN realizations to first-order DHM. The standard deviation of the WGN realizations was assigned as a percentage of the uncorrupted DHM dynamics (5%, 50%, 100%, or 150%). Results, reported in Table I, show that  $R_t$  is 100% provided that the standard deviation of the WGN is below 100%. Since irreversible dynamics are more likely to be detected at higher  $L$ ,  $R_t$  increases in Table I as a function of  $L$ .

V. SIMULATED DATA: TWO-LOOP NEGATIVE FEEDBACK MODEL

The fourth type of simulation is devoted to emphasizing the need of an irreversibility test for high-dimensional dynamics generated by models producing different dominant time scales via multiple delayed feedback loops. Let us consider the two-loop negative feedback model [14] described by the delayed differential equation

$$\dot{P}(t) = -P(t) + \frac{1}{2} \sum_{i=1}^2 \frac{\theta_i^n}{\theta_i^n + P^n(t - \tau_i)}. \tag{4}$$

We set  $n=45$ ,  $\theta_1=0.634$ , and  $\theta_2=0.704$ , with delays  $\tau_1=0.26$  and  $\tau_2=2.00$  and integration step of 0.001, thus generating a quasiperiodic dynamics [14]. The series was downsampled with a downsampling factor of 50 and sequences of

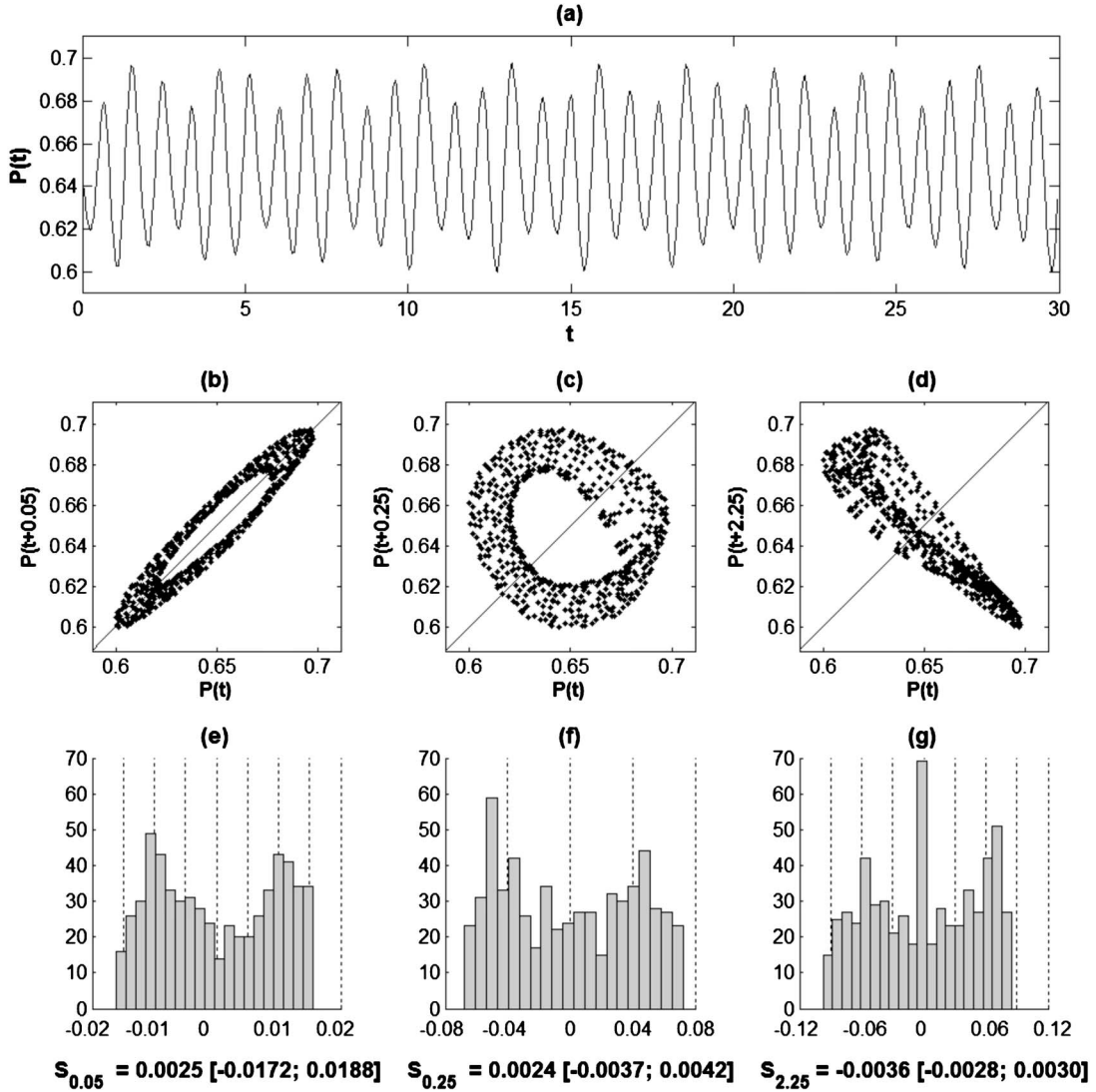


FIG. 3. Quasiperiodic dynamics obtained from the two-loop delayed feedback model (a). Scattergrams of  $P(t+0.05)$  vs  $P(t)$  (b),  $P(t+0.25)$  vs  $P(t)$  (c),  $P(t+2.25)$  vs  $P(t)$  (d); distributions of  $P(t+0.05)-P(t)$  (e),  $P(t+0.25)-P(t)$  (f), and  $P(t+2.25)-P(t)$  (g) with their skewness and the interval of skewness derived from surrogates.

about 600 samples were considered. This signal exhibits two clearly different temporal scales [see Fig. 3(a)]: the faster with a period of about 0.9, while the slower is exhibited with a period more than three times larger.

Figure 3 shows the scattergrams in the planes  $(P(t), P(t+0.05))$ ,  $(P(t), P(t+0.25))$ , and  $(P(t), P(t+2.25))$ . The distributions of  $P(t+0.05)-P(t)$  and  $P(t+0.25)-P(t)$  are symmetric [Figs. 3(e) and 3(f)], while that of  $P(t+2.25)-P(t)$  is asymmetric [Fig. 3(g)]. This simulation suggests that, given a model showing two dominant time scales (one faster and one slower), these two time scales might show different degrees of reversibility. Indeed, the distribution of  $P(t+\delta_t)-P(t)$  is asymmetric only when  $\delta_t$  ranges between 2.20 and 2.40, thus linking irreversibility to the slower time scale. On the contrary, the faster time scale, which needs a time shift  $\delta_t$  much smaller to be correctly resolved, is not detected as irreversible.

## VI. HEART PERIOD VARIABILITY DATA

We applied the proposed irreversibility test to the heart period ( $T$ ) beat-to-beat series (200–300 cardiac beats) derived from 26 young healthy humans undergoing to two different protocols. Ten subjects (ages ranging from 24 to 32) underwent recordings at rest and during 80° head-up tilt. Sixteen subjects (ages ranging from 21 to 35) underwent recordings at rest and standing. ECG (lead II) was sampled at 300 Hz (12-bit precision).  $T$  was derived as the temporal distance between two consecutive  $R$  peaks of ECG signal. Stationarity of the series was tested as reported in [23].

Figure 4 shows an example of the  $T$  irreversibility analyses for series taken from a subject during tilt and standing.  $T$  series during tilt has a skewness index ( $S_1=0.0368$ ) out of the 500 surrogate interval  $[-0.0164; 0.0137]$  being two irreversible. Indeed, the distribution of  $T(i+1)-T(i)$  is asymmetric with respect to 0 [Fig. 4(d)]. On the contrary, the null



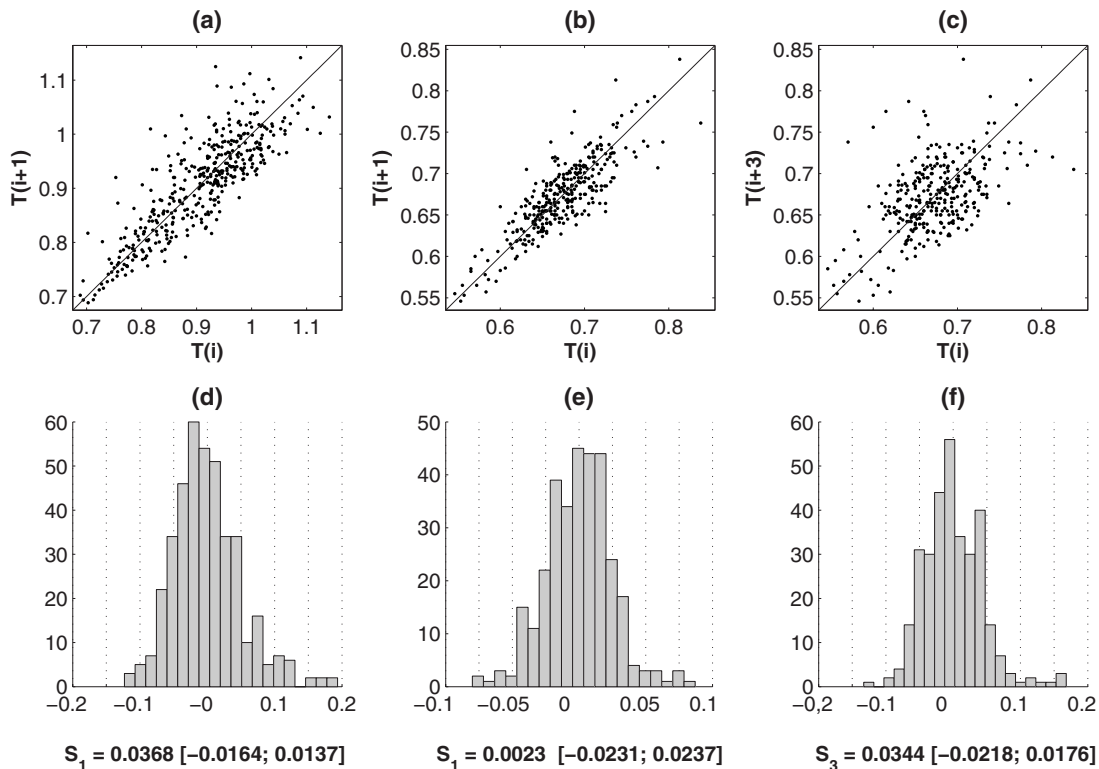


FIG. 4. Scattergrams of  $T(i+1)$  vs  $T(i)$  during tilt (a),  $T(i+1)$  vs  $T(i)$  during standing (b), and  $T(i+3)$  vs  $T(i)$  (c) during standing; distributions of  $T(i+1)-T(i)$  during tilt (d),  $T(i+1)-T(i)$  during standing (e),  $T(i+3)-T(i)$  during standing (f) with their skewness and the interval of skewness derived from surrogates.

hypothesis of reversibility in the plane  $(T(i), T(i+1))$  cannot be rejected in the case of the  $T$  series during standing. Indeed, the distribution of  $T(i+1)-T(i)$  is symmetric with respect to 0 [Fig. 4(e)] with  $S_1=0.0023 \in [-0.0231; 0.0237]$ . The same series is found irreversible in the plane  $(T(i), T(i+3))$  ( $S_3=0.0344 \notin [-0.0218; 0.0176]$ ), thus being four irreversible. Indeed, distribution of  $T(i+3)-T(i)$  is asymmetric with respect to 0 [Fig. 4(f)].

Figure 5 shows the percentages of  $L$ -irreversible  $T$  series in each experimental condition. The bars indicate the percentage of  $L$ -irreversible dynamics with  $L=5$  (the solid part of the bars represents the percentage of  $L$ -irreversible dynamics with  $L=2$ ). The percentage of two-irreversible dynamics during rest was similar to that during standing, while it increased during tilt. On the contrary, during standing the percentage of five-irreversible  $T$  series increased with respect to rest and became similar to that during tilt.

## VII. DISCUSSION

Simulations relevant to the delayed Henon map and the two-loop negative feedback clearly demonstrated that irreversibility analysis cannot be carried out at arbitrary fixed and/or low  $L$ . Indeed, the presence of a delay in the underlying generation mechanism might produce a displacement of irreversibility toward higher phase space dimensions. In other words, reversible temporal scales might coexist with irreversible temporal scales that need higher-dimensional phase spaces to be completely unfolded and only the expo-

ration of progressively increasing  $L$  guarantees the correct evaluation of this dynamical property. In addition, simulations relevant to reversible processes (i.e., WGN or colored noises) indicated that the percentage of false rejections increases with  $L$  (i.e., it is more likely to erroneously detect irreversible dynamics at large  $L$ ). Therefore, it is mandatory to adopt theoretical functionals that keep low the probability of false rejections and/or to increase the level of confidence of the surrogate data test. Simulations relevant to nonlinear delayed dynamics corrupted by reversible noise (i.e., WGN) suggested that the proposed test is quite robust with respect to noise.

The short-term analysis of  $T$  variability indicated that the  $T$  series is irreversible with  $L=2$  in 25% and 27% of subjects at rest and during standing, respectively [7,24].

The increase of irreversible dynamics when passing from  $L=2$  to  $L=5$  is important both at rest and during standing, thus rendering mandatory the use of an irreversibility test that explores progressively increasing embedding dimensions. It is worth noting that the increase of irreversible dynamics when passing from  $L=2$  to  $L=5$  is more important during standing. This phenomenon might be related to the increased phase shift in the closed-loop baroreflex regulation observed during this experimental condition. Indeed, during standing the phase between the  $T$  and arterial pressure becomes more negative at the respiratory rate [25], thus indicating that the beat-to-beat interactions along the baroreflex loop do not occur in the same cardiac beat as at rest but with a delay of one or more beats. The increase of the delay in the beat-to-beat domain between  $T$  and arterial pressure has been

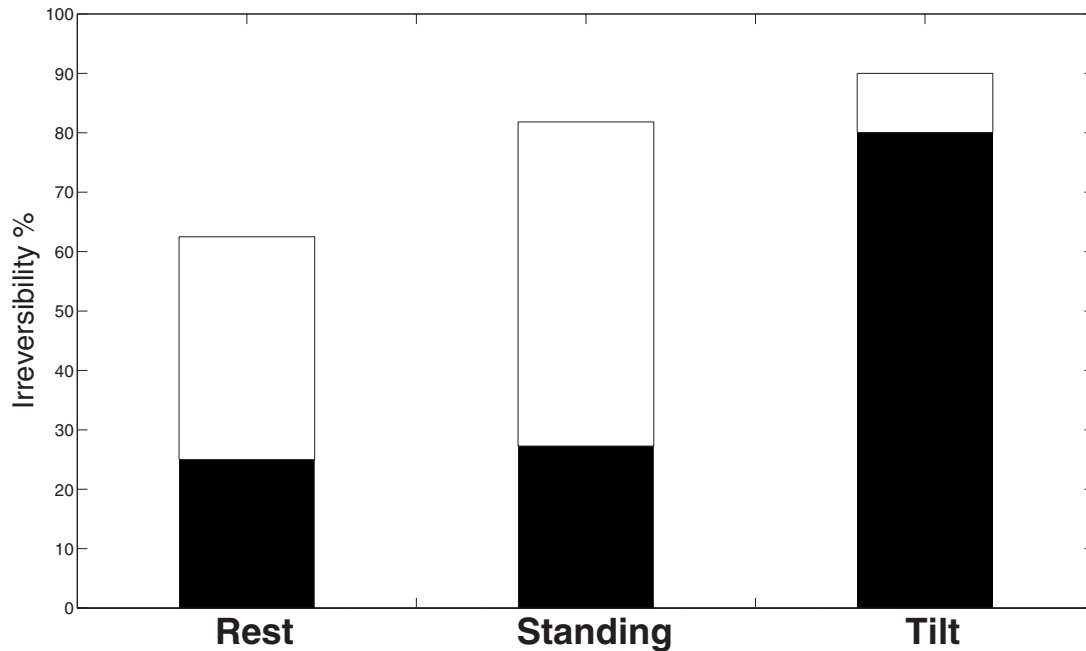


FIG. 5. Bar graph representing the percentage of five-irreversible dynamics relevant to the analysis of  $T$  series at rest, during standing and tilt. The solid bars indicate the percentage of two-irreversible dynamics.

observed in several experimental conditions characterized by sympathetic activation such as during lower body negative pressure [17], thus supporting the need to look at higher phase space dimensions during these conditions. Tilt is another experimental condition characterized by a sympathetic activation. Since  $T$  variability exhibits an important percentage of  $L$ -irreversible dynamics with  $L=2$  [7,24], the increase of this percentage as a function of  $L$  is not very important. The larger presence of  $L$ -irreversible dynamics with  $L=2$  during tilt than during the sympathetic activation produced by standing might be due to the larger importance of the sympathetic activation during tilt that reduces the complexity of  $T$  variability [26] and renders irrelevant the exploration of higher-dimensional phase spaces. Indeed, during tilt power spectrum exhibits only a dominant peak in the low-frequency band [27], while during standing the power spectrum of heart period variability is characterized by two clear peaks, in the low- (from 0.04 to 0.15 Hz) and high-frequency (around the respiratory rate) bands [28].

In conclusion, we tested the hypothesis that, in the presence of a signal characterized by at least two dominant time scales (e.g., quasiperiodic dynamics generated by a two-loop negative feedback or short-term heart rate variability), temporal scales characterized by different degrees of irreversibility might coexist. In the presence of an increased delay in the underlying closed-loop regulatory mechanisms and of complex dynamics characterized by several (more than two) dominant temporal scales, it is advisable to test irreversibility by exploring progressively increasing embedding dimensions since irreversibility might be shifted toward slower time scales.

#### ACKNOWLEDGMENTS

We gratefully acknowledge support from the CAPES/Brazil, FIRST 2005 grant, University of Milan, and Italian Space Agency DCMC Project.

- 
- [1] C. Diks *et al.*, Phys. Lett. A **201**, 221 (1995).
  - [2] M. J. van der Heyden, Phys. Lett. A **216**, 283 (1996).
  - [3] T. Schreiber and A. Schmitz, Physica D **142**, 346 (2000).
  - [4] B. P. T. Hoekstra *et al.*, Chaos **7**, 430 (1997).
  - [5] I. Prigogine and I. Antoniou, Ann. N. Y. Acad. Sci. **879**, 8 (1999).
  - [6] M. Costa, A. L. Goldberger, and C.-K. Peng, Phys. Rev. Lett. **95**, 198102 (2005).
  - [7] A. Porta *et al.*, Comput. Cardiol. **33**, 77 (2006).
  - [8] P. Guzik *et al.*, Biomed. Tech. **51**, 272 (2006).
  - [9] C. L. Ehlers *et al.*, J. Neurosci. **18**, 7474 (1998).
  - [10] C. Braun *et al.*, Am. J. Physiol. **275**, H1577 (1998).
  - [11] M. C. Mackey and L. Glass, Science **197**, 287 (1977).
  - [12] H. P. Koepchen, in *History of Studies and Concepts of Blood Pressure Waves*, edited by K. Niyakawa, C. Polosa, and H. P. Koepchen (Springer, Berlin, 1984), pp. 3–23.
  - [13] D. Hoyer *et al.*, Chaos **17**, 015110 (2007).
  - [14] J. C. Bastos de Figueiredo, L. Diambra, L. Glass, and C. P. Malta, Phys. Rev. E **65**, 051905 (2002).
  - [15] G. Nollo *et al.*, Am. J. Physiol. Heart Circ. Physiol. **283**, H1200 (2002).
  - [16] C. Borst *et al.*, J. Auton. Nerv. Syst. **9**, 399 (1983).

- [17] A. P. Blaber *et al.*, *Am. J. Physiol.* **268**, H1688 (1995).  
[18] W. H. Cooke *et al.*, *J. Physiol.* **517**, 617 (1999).  
[19] F. Takens, in *Dynamical Systems and Turbulence*, Lecture Notes in Mathematics edited by D. Rand and L. S. Young (Springer-Verlag, Berlin, 1981), Vol. 366, pp. 366—381  
[20] J. Theiler *et al.*, *Physica D* **58**, 77 (1992).  
[21] G. Weiss, *J. Appl. Probab.* **12**, 831 (1975).  
[22] D. T. Kaplan *et al.*, *Biophys. J.* **59**, 945 (1991).  
[23] A. Porta *et al.*, *Comput. Cardiol.* **31**, 645 (2004).  
[24] K. R. Casali *et al.*, *FASEB J.* **A564**, 612.8 (2007).  
[25] A. Porta *et al.*, *Comput. Cardiol.* **31**, 265 (2004).  
[26] A. Porta *et al.*, *J. Appl. Physiol.* **103**, 1143 (2007).  
[27] N. Montano *et al.*, *Circulation* **90**, 1826 (1994).  
[28] D. Lucini *et al.*, *J. Hypertens.* **18**, 281 (2000).